Journal of The Electrochemical Society, **155** (2) B119-B124 (2008)
0013-4651/2007/155(2)/B119/6/$23.00 © The Electrochemical Society

Durability of Perfluorosulfonic Acid and Hydrocarbon Membranes: Effect of Humidity and Temperature

Vijay A. Sethuraman,[a,c,*] John W. Weidner,[a,,z] Andrew T. Haug,[b,d,**] and Lesia V. Protsailo[b,**]**

[a]*Department of Chemical Engineering, Center for Electrochemical Engineering, University of South Carolina, Columbia, South Carolina 29208, USA*
[b]*UTC Power, South Windsor, Connecticut 06074, USA*

The effect of humidity on the chemical stability of two types of membranes [i.e., perfluorosulfonic acid type (PFSA, Nafion 112) and biphenyl sulfone hydrocarbon type, (BPSH-35)] was studied by subjecting the membrane electrode assemblies (MEAs) to open-circuit voltage (OCV) decay and potential cycling tests at elevated temperatures and low inlet-gas relative humidities. The BPSH-35 membranes showed poor chemical stability in ex situ Fenton tests compared to that of Nafion membranes. However, under fuel cell conditions, BPSH-35 MEAs outperformed Nafion 112 MEAs in both the OCV decay and potential cycling tests. For both membranes, (*i*) at a given temperature, membrane degradation was more pronounced at lower humidities and (*ii*) at a given relative humidity operation, increasing the cell temperature accelerated membrane degradation. Mechanical stability of these two types of membranes was also studied using relative humidity (RH) cycling. Due to decreased swelling and contraction during wet-up and dry-out cycles, Nafion 112 lasted longer than BPSH-35 membranes in the RH cycling test.
 [DOI: 10.1149/1.2806798]

Manuscript submitted July 9, 2007; revised manuscript received October 12, 2007. Available electronically December 3, 2007.

Current engineering requirements for automotive fuel cells demand stack operation at higher temperatures (>100°C) and low relative humidities (RH) (<25% RH). Elevated temperature operation offers better tolerance to CO and better water and thermal management, enabling easier system integration. Lower RH operation offers quicker start-ups and better freeze-cycle management. The current benchmark membrane for proton exchange membrane (PEM) fuel cells is Nafion, a perfluorinated sulfonated copolymer made by DuPont.[1] Nafion copolymers exhibit good thermal and chemical stability as well as high proton conductivity under hydrated conditions at temperatures below 90°C. However, applications of these membranes are limited at high temperatures and low RH due to their loss of conductivity.[2] These limitations have led to the search for new polymer electrolytes for PEMs. Extensive reviews of polymer-based PEMs have recently been published.[3,4] In searching for new polymer electrolytes for use in PEM fuel cells, it is a common practice to functionalize aromatic polymers with proton conducting groups. Promising candidates for an alternative high-temperature and low-humidity PEMs are derived from poly(arylene ether sulfone)s,[5] well-known engineering thermoplastic materials (particularly when devoid of aliphatic units) that display excellent thermal and mechanical properties. Sulfonated poly(arylene ether sulfone)s are synthesized by attaching sulfonic acid groups in polymer modification reactions (postsulfonation route) and have been investigated since the pioneering work of Noshay and Robeson,[6] who developed a mild sulfonation procedure for the commercially available bisphenol-A-based-poly(ether sulfone). Because these sulfonated polymers exhibited protonic conduction, they were first used in desalination membranes for reverse osmosis.

McGrath and his group synthesized aromatic, film-forming, highly sulfonated poly(arylene ether sulfone) copolymers (also known as bi-phenyl sulfone-H form or BPSH-XX) via direct copolymerization for use in PEM fuel cells.[7] The XX represents the molar fraction of sulfonic acid units in the copolymer repeat unit. These aromatic ionomers are copolymers that are comprised largely of repeating thermally stable aromatic rings, which are stiffer, longer, and have higher glass transition temperatures than Nafion and yet are designed to produce ductile films. They have shown that direct copolymerization has many advantages such as enhanced stability, control of ion-contaminating sites, a whole variety of molecular structures, and the ability to make higher molecular weights, which translate to improved mechanical properties.[3] These polymers showed much higher yield strength and modulus than the analogous perfluorinated copolymers.[3]

Membrane degradation in the PEM fuel cell environment has been discussed[8] as having chemical and mechanical components. In this work, the chemical and mechanical stability of two types of membranes, [i.e., perfluorosulfonic acid type (PFSA, Nafion 112) and biphenyl sulfone hydrocarbon (or H^+) type, (BPSH-35)] is studied.[e] Chemical stability was studied using ex situ Fenton test[9,10] and in situ OCV decay[11] and potential cycling tests[12,13] with H_2/O_2 feed at elevated temperatures and low RH. The mechanical stability of these two membranes was studied by RH cycling at elevated temperatures.

Experimental

Fuel cell construction.— Commercially available Pt/C catalyst (TEC10E50E 46.7% Pt on Ketjen black carbon, Tanaka Kikinzoku Kogyo KK, Japan) was mixed with Nafion [5% aqueous solution, 1100 equivalent weight (EW); Solution Technology Inc., Mendenhall, PA] ionomer, and the resulting catalyst-ionomer ink (79% catalyst, 21% Nafion) was coated onto Teflon-based (EI DuPont de Nemours and Company) decals. These catalyst-coated decals were dried in N_2 at room temperature (~25°C) and atmospheric pressure for 30 min. Catalyst-coated membranes (CCMs), 6.5 × 6.5 cm, were then made by hot pressing the catalyst-coated Teflon decals onto both sides of Nafion 112 membranes (proton form) at 130°C and 2040 kg for 300 s. Reinforced silicon, unreinforced silicone, and Teflon pads were used as gaskets and supports for this process. The CCMs had a Pt loading of ~0.4 mgPt/cm^2 on both anode and cathode sides.

The CCM was assembled into a fuel cell (25 cm^2 hardware, Fuel Cell Technologies Inc., Albuquerque, NM). Wet-proofed Toray paper with a microporous layer was used as gas diffusion media (GDM). Untreated Toray paper (TGP-H-60, 190 μm thick, Toray Industries, Japan)[14] was wet-proofed (prior to the application of the microporous layer) in house by briefly immersing them in a 10% aqueous Teflon solution followed by drying in room temperature for 24 h. A microporous layer, approximately 25 μm thick, containing

* Electrochemical Society Student Member.
** Electrochemical Society Active Member.
[c] Present address: Environmental Energy Technologies Division, Lawrence Berkeley National Laboratory, Berkeley, California 94720.
[d] Present address: 3M Center, 3M Fuel Center Components, St. Paul, MN 55144.
[z] E-mail: weidner@engr.sc.edu

[e] BPSH-35 membranes were obtained from Professor James E. McGrath, Department of Chemistry, Virginia Polytechnic Institute and State University, Blacksburg, VA 24061.

graphite (Vulcan XC-72) and 10 wt % Teflon was added to the wet-proofed Toray paper. The total thickness of the GDM was 243 μm. Gaskets (of varying thicknesses) were chosen in such a way that they allowed for 21% compression on the GDMs at 5.1 N m of torque on the bolts. The fuel cell had nonporous modular serpentine flow channels on the anode side and interdigitated flow channels on the cathode side. The graphitic flow-channel blocks had the same dimensions as the end plates. The assembled fuel cell was tested for throughput, gas crossover, and overboard leaks and then conditioned with H_2/O_2 (anode/cathode) in a fuel cell test stand (Habco Inc., CT) at 80°C and 101 kPa (absolute). Several current-voltage (*I-V*) curves were measured in hydrogen and oxygen with 30 and 25% utilizations, respectively, until a steady high performance was reached. The following durability experiments were then performed for Nafion 112 and BPSH-35 membranes.

Open-circuit voltage decay test.— After the cell was conditioned, it was put on open-circuit voltage (OCV) with H_2/O_2 as feed gases on the anode/cathode sides, respectively. The OCV decay was monitored over the life of the cell until it failed. Failure criterion was defined as an OCV of 0.8 V or below or a hydrogen crossover current of 10 mA/cm^2, whichever occurred earlier. The pressure of the fuel cell system was set such that the gases had a fixed partial pressure regardless of their humidity. The OCV decay test was briefly interrupted every 24 h for performing some diagnostics (described below) to evaluate the condition of the fuel cell. The tests were performed as a function of temperature (80–120°C) and RH (25–100% RH). A new membrane electrode assembly (MEA) was used for each OCV decay test.

Potential cycling.— Potential cycling was performed using a potentiostat (M273A, Princeton Applied Research Inc., Oak Ridge, TN) in which the fuel cell cathode (O_2) was cycled between open circuit and a fixed current of 25 mA/cm^2 for 1 min each (i.e., duty cycle = 0.5). Potential cycling test was carried out for different temperatures and RH. A new MEA was used for each potential cycling test.

Membrane humidity cycling.— A membrane with no catalyst on either side was built into a fuel cell apparatus with gas-diffusion layers and appropriate gaskets on both sides. The gas-diffusion layers were not coated with a microporous layer because the presence of a microporous layer would act as an additional resistance to water transport between the gas channels and the membrane and would slow the wetting and the drying of the membrane.[15] 100% humidified N_2 [at 1000 cm^3 min^{-1} total at standard temperature, pressure (STP); UHP, Praxair] was fed to both sides of the membrane for 1 h followed by the same rate of dry N_2 (i.e., humidity bottles were bypassed) for the next hour. This induced periodic mechanical stresses to the membrane. Physical gas (N_2) crossover (at ΔP = 20.68 kPa) was measured and water samples were collected at regular intervals to diagnose the state of the membrane. The cell was cycled until the gas crossover measured more than 500 cm^3 min^{-1}.

Hydrogen crossover measurements.— Molecular hydrogen crossing over from the anode side to the cathode side of the membrane was measured using a potential sweep between 0 and 500 mV vs dynamic hydrogen electrode (DHE) on the cathode with N_2 flowing over it. While the magnitude of the oxidation current in the voltammogram gave an indication of the amount of H_2 crossing over, the slope of the *I-V* curve gave an indication of the electrical resistance across the two electrodes (commonly known as "short"). A well-shorted electrode would mean that the electrodes were well insulated electronically (i.e., zero slope) and a poorly shorted electrode would mean that the electrodes were physically in contact with each other (i.e., infinite slope). A high H_2 crossover was an indication of membrane degradation or expanding pinholes and a poor short was an indication of carbon strands from either electrode in physical contact with each other.

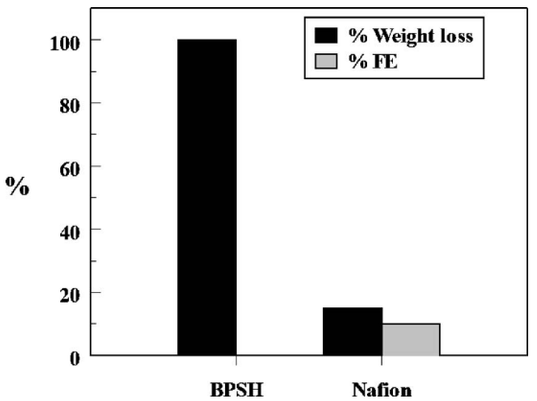

Figure 1. Percent weight loss and fluorine emission obtained from Fenton tests on BPSH and Nafion membranes after 24 and 96 h, respectively.

Fluorine and sulfur emission rates.— Water samples were collected once every 4 h during the first 16 h of the OCV decay and potential cycling experiments. After that, they were collected every 24 h until cell failure. These water samples and the leachate from the Fenton tests were analyzed for the presence of fluorine and sulfur using a Dionex ICS-200 ion chromatography system.

Fenton tests.— A Nafion 112 membrane (H^+ form, DuPont Fluoroproducts, Fayetteville, NC) sample measuring ~2 × 2 in. was cut and heated in a clean glass vial containing water at 80°C for 2 h to remove any surface impurities and solvents. The water was later drained from the vial and the membrane was dried in vacuum at 80°C for 4 h. The dry weight of the membrane was then measured. This weight was used to prepare ferrous sulfate solution such that it contained 25 mg Fe/g Nafion in 500 mL water. $FeSO_4 \cdot 7H_2O$ (98.1% assay, Fischer Scientific Company, Fairlawn, NJ) was used for this purpose. The dried Nafion membrane was placed in this solution for 15 h in a N_2 atmosphere. This process impregnated Fe ions into the membrane. After this impregnation process, the membrane was dried in vacuum at 80°C for 4 h. The dry weight of the membrane impregnated with Fe ions was measured.

The Fe impregnated membrane was placed in a Teflon container containing 100 mL of 3% hydrogen peroxide aqueous solution (30%, VWR International) at 80°C. Because hydrogen peroxide decomposes in the presence of a metal, this solution was replaced once every 24 h and the leachate was saved for fluorine analysis. After 96 h, the membrane was dried in vacuum at 80°C for 4 h. The weight loss, if any, was recorded. This process was repeated with a sample of hydrocarbon membrane. The leachate was analyzed for fluorine using a Dionex ICS-200 ion chromatography system.

Linear expansion and swelling.— Nafion 112 and BPSH-35 membrane samples were cut into 2 × 2 cm pieces. They were placed in a vacuum oven at 25°C for 30 min. Their initial dimensions were measured immediately after taking them out of the vacuum oven at 25°C using a Mitutoyo digital caliper (i.e., length, width) and screw gauge (thickness). The membrane samples were then immersed in water at 25°C and left there for 30 min. Next, the samples were taken out and their dimensions were measured again and recorded. The samples were then placed in boiling water for a period of 10 min and their dimensions recorded afterwards. The increase in thickness due to swelling was estimated by subtracting the measured thickness after boiling at 80°C from the initial thickness measured at 25°C.

Results and Discussion

Chemical stability.— Figure 1 shows percent weight loss and percent fluorine emission after Fenton tests on Nafion 112 and BPSH-35 membranes. Percent fluorine emission is defined as the

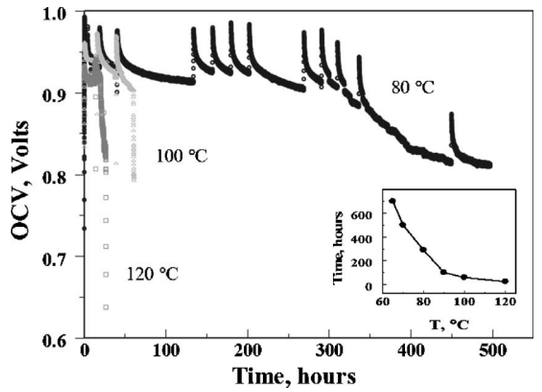

Figure 2. OCV decay for Nafion 112 MEA operating on H_2/O_2 and 25% RH at 80, 100, and 120°C. Inset: Nafion 112 MEA life at OCV decay tests until failure (i.e., OCV ≤ 0.8 V) at 25% RH for various temperatures.

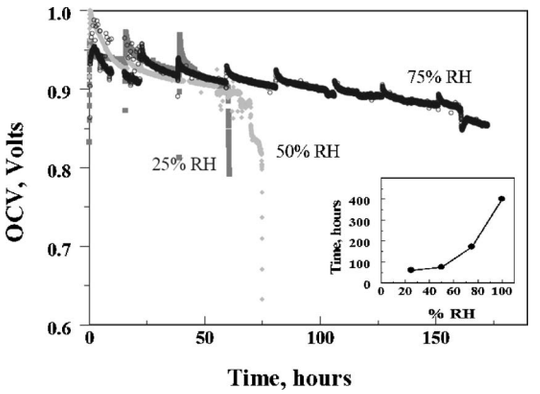

Figure 3. OCV decay for Nafion 112 MEA operating on H_2/O_2 at 100°C and 150 kPa for the following inlet gas humidities: 25, 50, and 75% RH. Inset: Nafion 112 MEA life at OCV decay tests until failure (i.e., OCV ≤ 0.8 V) at 100°C for different RH.

ratio of fluoride ions measured in the leachate solution to the original amount of fluorine in the Nafion 112 membrane sample. The Nafion 112 sample showed much higher chemical stability and lost 16% (by weight) after 96 h. For the Nafion 112 sample, the weight loss estimated by gravimetric procedure correlated well with fluorine content from the leachate within the timescale of this experiment (i.e., initial stages of degradation). For this, approximately two-thirds of membrane (by weight) was assumed to be fluorine. For example, the estimated weight loss based on the measured fluoride ion concentration in the leachate was 14.6% after 96 h. This is in accordance with previously observed[16] stability of the Nafion membrane in Fenton solution test media. BPSH-35 turned yellow soon after the start of the Fenton test and split into pieces after 16 h. The sample disintegrated completely after 24 h. In order to obtain a measurable weight loss from the Fenton tests on BPSH-35 samples, the impregnation loading was systematically reduced coupled with a reduction in the concentration of H_2O_2 solution. At 1 mg $FeSO_4$/g membrane loading, 4.75% weight loss was observed after 4 h. BPSH-35 samples with no impurity impregnation also disintegrated in 3% H_2O_2 solution after 125 h.

Figure 2 shows the result of the OCV decay test on a Pt/KB-coated Nafion 112 membrane operating on H_2/O_2 at 25% RH for three different temperatures. The inset shows membrane life as a function of temperature at 25% RH operation with H_2/O_2 feed. The OCV profiles have spikes because the cell was periodically stopped for performing hydrogen crossover measurements. Because these diagnostics involved scanning the cathode between 50 and 1150 mV vs DHE, they resulted in the reduction of Pt oxides to Pt on the cathode. This temporary increase in the availability of metallic Pt increased the open-circuit potential when the OCV decay test was resumed. The voltage decayed back to the voltage prior to interruption once oxides were reformed. The overall OCV decay rates were found to be independent of the number of times the cell was stopped for diagnostics. The cell operating at 120°C failed in less than 25 h, while the cells operating at 100 and 80°C failed after 56 and 498 h, respectively.

Figure 3 shows the result of the OCV decay test on a Pt/KB-coated Nafion 112 membrane operating on H_2/O_2 at 100°C for three different gas humidities. The cell operating at 25% RH failed after 56 h, while the cells operating at 50 and 75% RH failed after 75 and 175 h, respectively. Healy et al.,[10] Knights et al.,[17] and Endoh et al.[18] all observed higher degradation under low humidity conditions. Data trends from Fig. 2 and 3 indicate that membrane degradation significantly increases when a combination of high-temperature and low-humidity conditions exist. At least two phenomena explain this behavior: (*i*) the water-dependent glass-transition temperature of Nafion and (*ii*) the humidity and temperature-dependent peroxide formation rates as reported earlier.[19,20] Nafion is a homopolymer and exhibits three glass transitions according to Yeo and Eisenberg[21]: an α transition at 111°C due to the movement of the poly(tetrafluoroethylene) (PTFE) backbone, a β transition at 23°C due to the relaxation of the ionic regions, and a γ transition at −110°C due to local short-range motions of fluorocarbons in the PTFE backbone. Later findings by Kyu and Eisenberg[22] on the sensitivity of the α peak to the change in the water content of the membrane suggest that this assignment of α and β peaks be reversed. This humidity-dependent α transition plays an important role in the viscoelastic behavior and hence the glass-transition temperature of Nafion. The lower the water content, the lower the glass-transition temperature, with completely dry Nafion approaching the reported $T_{g,\alpha}$ = 111°C. Furthermore, X-ray diffraction (XRD) studies of Nafion showed that the characteristic peak (18° diffraction angle) greatly diminished under low-humidification conditions,[23] suggesting low humidification could decrease the crystallinity of Nafion. O_2 and H_2 diffusion coefficients for completely dry Nafion membrane were reported by Sakai et al.[24] to be two orders of magnitude greater than that for fully humidified Nafion membrane. Haug et al. measured gas permeabilities across Nafion as a function of temperature and RH.[25] According to them, the oxygen permeability across Nafion decreased by 50% when RH was decreased from fully saturated to 25%. Therefore, the initial lower OCV at lower humidity conditions is due to gas crossing the membrane and depolarizing the opposite electrode. The relatively faster OCV decay at lower-humidity conditions is due to increased rate of H_2O_2,[19] $OH^{\cdot}$, and $OOH^{\cdot}$[26] generation at lower-humidity conditions, which accelerate membrane degradation, resulting in performance decay. The H_2O_2 selectivity in oxygen reduction reaction was found to increase with a decrease in water activity (decrease in humidity).[20,21]

The OCV decay profiles show two slopes: (*i*) a slow decay followed by (*ii*) a rapid fall. The slow decay in the OCV is due to material loss from the membrane and its gradual thinning. The rapid fall in the OCV is due to (*i*) pin-hole formation resulting in extremely high gas crossover rates and/or (*ii*) shorting between carbon electrodes due to complete loss of membrane mass. Evidence for the former can be seen in Fig. 4, where the rapid fall in the OCV coincides with a rise in hydrogen crossover current. The difference between the former and the latter slopes was more pronounced at lower humidities. The OCV decay rate was measured as the ratio of the difference between the initial OCV and the OCV prior to the rapid fall to the time between these two OCVs. The OCV decay rates are summarized in Table I for different temperatures and RH. At 100°C and 25% RH operation, the OCV decay rate measured from a BPSH-35 cell (Fig. 5) is approximately three times lower than a similar Nafion 112 cell.

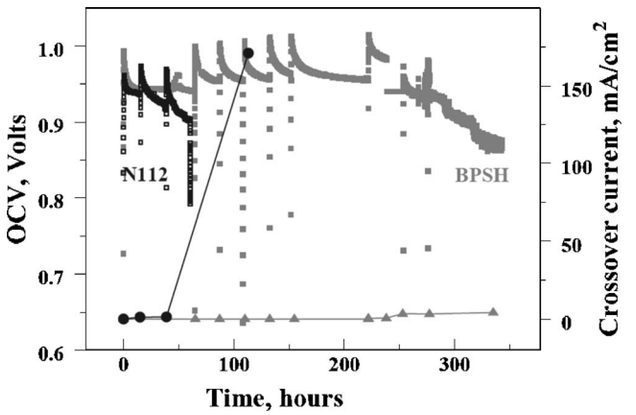

Figure 4. OCV decay (□, ■) and hydrogen crossover current (●, ▲) for Nafion 112 (□, ●) and BPSH (■, ▲) membranes at 100°C and 25% inlet gas relative humidity.

Figures 4 and 5 show the comparison between the performances of Nafion 112 and BPSH-35 membranes during the OCV decay experiment and potential cycling experiments, respectively, at 100°C and 25% RH conditions. Only the OCV data is shown for the case of potential cycling test in Fig. 6. The OCV decay rate of BPSH cell was less than that of Nafion 112 cell in both cases. Unlike the OCV decay test, there is no rapid fall in the OCV at any point during the potential cycling tests. At 100°C and 25% RH operation, Nafion 112 lasted three times (~175 h) longer during the potential cycling test than during the OCV decay test (~60 h). This result seems counterintuitive because potential cycling should degrade the cell faster than maintaining at open-circuit potential. Potential cycling an oxygen cathode creates potentials that favor peroxide formation, i.e., the cathode routinely experiences potentials in the 0.4–0.7 V vs NHE window. Also unlike the OCV decay test, potential cycling eliminates continuous passivation of Pt, i.e., less PtO^- and $PtOO^-$ leads to more Pt dissolution, thereby increasing the concentration of Pt^{2+} in the cathode. However, during potential cycling, water production at the cathode during load intervals increases the local water activity. This increase in local water activity decreases both peroxide production and Pt dissolution. Second, potential cycling interrupts oxygen crossover to the anode because oxygen is consumed during load intervals. Therefore, the net flux of O_2 to the anode side would be lower during potential cycling than during the OCV decay test. Lower O_2 flux would mean lower peroxide production at the anode. Third, the cathode experiences lesser time at Pt dissolution potentials. Comparison between these two membranes in terms of H_2 crossover across the membrane is also shown in these figures. Similar to the OCV decay profile, the H_2 crossover current also does not show a sudden increase at any time during the potential cycling test.

The OCV decay rate of a cell is a measure of the chemical stability of its MEA. The membranes typically fail during the OCV decay test due to material loss, resulting in overall thinning of the membrane or pinhole formation, both of which cause gas crossover

Table I. Voltage decay rates for Nafion 112 and BPSH-35 membranes measured during OCV decay experiments.

Membrane	Temperature (°C)	% RH	OCV decay rate (mV/h)
Nafion 112	80	25	0.358
	100	25	1.82
		50	1.064
		75	0.498
	120	25	4.02
BPSH-35	100	25	0.507

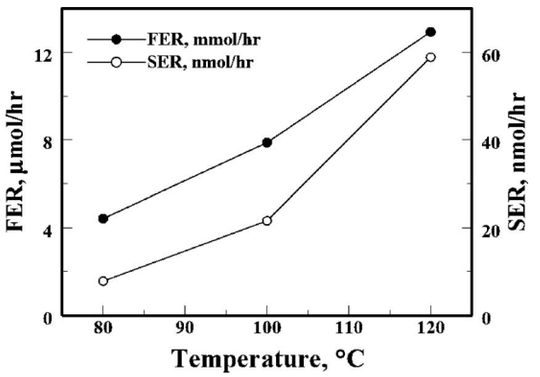

Figure 6. Total average fluorine (●) and sulfur (○) emission rates for a Nafion 112 membrane during OCV decay as a function of temperature.

and electrical shorting. The total fluorine and sulfur emission rates, defined as the ratio of total moles of fluorine or sulfur emitted to the total membrane life, exhibits linear dependence vs temperature at low-humidity operation. Both gas crossover and electrical shorting lead to a drop in the OCV. The loss of fluorine and sulfur as measured in the exhaust water (Fig. 6) confirms that the Nafion membrane is losing mass, and post-test images from the cycling tests (Fig. 7) reveal that significant thinning occurred to the Nafion membrane during these accelerated tests. Nafion 112 lost 30 μm (60%) of its thickness in 100 h of potential cycling between open circuit and 25 mA cm^{-2} at 100°C and 25% RH. However, BPSH-35 membrane did not thin during the same test for over 300 h. Sulfur emission from BPSH-35 cell was very insignificant and its measurement was discontinued. It is clear from these in-cell accelerated chemical-stability tests that BPSH-35 out-performs Nafion 112. Though Fenton tests indicate that the BPSH-35 membranes degrade strongly in the presence of trace iron contamination, they do not translate to their stability in the OCV decay tests. Conversely, good chemical stability exhibited by Nafion 112 membranes during Fenton tests did not translate to their in-cell stability. Details of Fenton test applicability and its discrepancy with in-cell accelerated membrane degradation tests are explained elsewhere.[27]

If the membrane degradation occurs via peroxy-radical attack, as reported by Cleghorn et al.,[28] then the reason for the above performances could be because of the gas-permeation properties of these membranes. Oxygen permeability, measured using electrochemical monitoring technique, is much higher for a Nafion 112 membrane

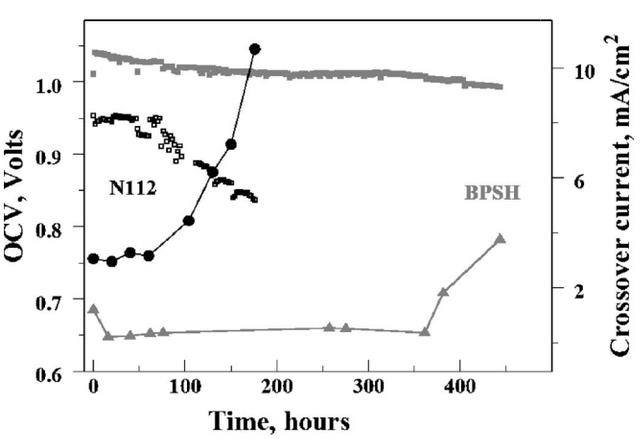

Figure 5. OCV (□, ■) and hydrogen crossover current (●, ▲) for Nafion 112 (□, ●) and BPSH (■, ▲) membrane during potential cycling (duty cycle = 0.5) between open circuit and 25 mA cm^{-2} (1 min each) at 100°C, 150 kPa, and 25% RH on H_2/O_2.

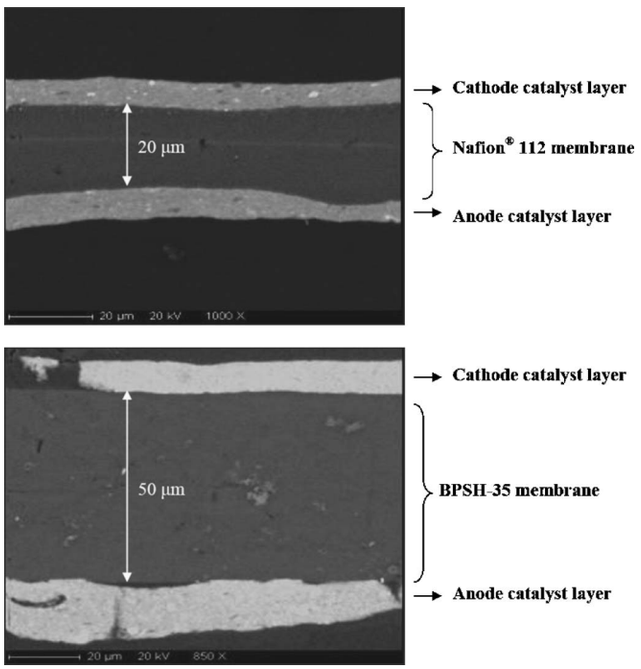

Figure 7. Post-test cross-sectional images of Nafion and BPSH-35 MEAs. The MEAs were cycled between open circuit and 25 mA/cm^2 for 1 min each at 100°C and 25% RH on H_2/O_2.

than a BPSH-35 membrane of equivalent thickness. This is shown in Fig. 8. Gas-permeation property of a membrane has two major implications to its durability in a PEM fuel cell, the transport of oxygen from the cathode side to the anode side and the transport of hydrogen from the anode side to the cathode side of a fuel cell. While the former affects hydrogen peroxide production, the latter plays a significant role in Pt deposition inside the membrane.

H_2O_2 formation occurs at the anode at OCV conditions because of the existence of a favorable local potential (~0 V vs NHE) and at both anode and cathode at load conditions. Because oxygen crossover rates are about 11 times lower for a BPSH-35 membrane compared to a Nafion 112 membrane, with the anode catalyst being the same, the former produces 11 times lower peroxide at its anode side than the latter at all conditions. It was shown earlier[19] that H_2O_2 formation in a fuel cell is sensitive to humidity and temperature. This partly explains why Nafion 112 showed poor chemical stability during in-cell tests at high temperatures and lower humidities.

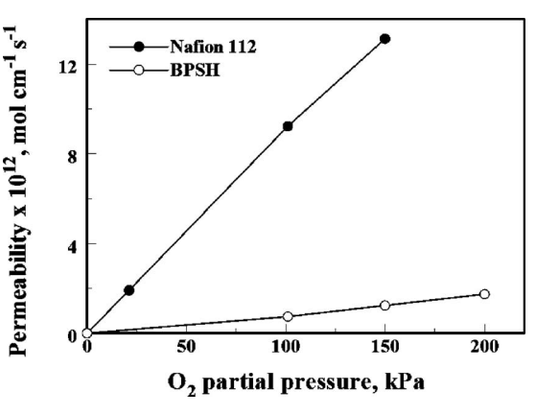

Figure 8. Oxygen permeability rates for Nafion 112 and BPSH membranes measured using the electrochemical monitoring technique at 25°C for different oxygen partial pressures.

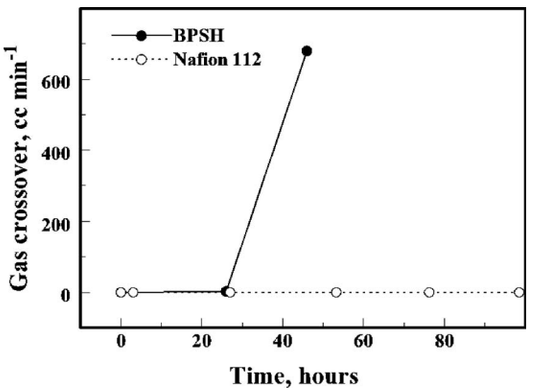

Figure 9. Gas crossover at 20.68 kPa differential nitrogen pressure across the membrane measured during the humidity cycling test on Nafion 112 and BPSH membranes. The RH was cycled between 100% for 1 h and 0% for 1 h at 100°C and 150 kPa.

Second, lower hydrogen transport from the anode side to the cathode side affects Pt deposition in the membrane. At high potentials normally experienced at the cathode during OCV conditions, Pt dissolves[29] from the support as Pt^{2+} and diffuses into the membrane because of concentration gradient. Molecular H_2 crossing over from the anode side acts as a reductant and reduces the Pt^{2+} species chemically, which results in the chemical deposition of metallic Pt inside the membrane.[30] Similar chemical platinization of Nafion has been reported earlier by Fedkiw et al.[31,32] and Takenaka et al.[33] The presence of Pt inside the membrane catalyzes the formation of hydroxyl radicals[27] which attack the membrane.[34] Assuming the rates of Pt dissolution and Pt^{2+} migration are the same for both BPSH-35 and Nafion 112 membranes, the former, due to its lower H_2 crossover, has a lower concentration of Pt inside the membrane than the latter.

Mechanical stability.— Mechanical stability of the membranes was tested by alternating completely dry feed gas and fully saturated (100% RH) feed gas at 1 h intervals. The membranes swell when soaked in water and shrink during drying. The repeated swelling and contraction experienced by the membrane during RH cycling induces mechanical stresses in the membrane, which may eventually lead to failure. Figure 9 shows gas crossover measured at 20.68 kPa at various time intervals during this RH cycling. Nafion 112 showed lower gas crossover and hence better mechanical stability than BPSH-35 membrane. This is in accordance with Mathias et al.,[35] who reported higher mechanical stability for a improved PFSA and Nafion 112 membranes than an aromatic hydrocarbon membrane based on RH cycling between 0% and 150% at 80°C. The increased expansion and contraction of the BPSH membrane compared to Nafion 112 during wet-up and dry-out cycles caused its failure. The failed BPSH-35 membranes had cracks along the edge of the gasket-membrane interface, where the stresses were maximal during expansion and contraction during RH cycling. Linear expansion in all three dimensions between completely dry and wet conditions was measured for Nafion and BPSH membranes and is tabulated in Table II. The in-cell and out-of-cell results were consistent.

Table II. Percent linear expansion in *x*, *y*, and *z* directions for Nafion 112 and BPSH membranes measured at 25°C and 1 atm.

Membrane	Linear expansion *x* direction (%)	Linear expansion *y* direction (%)	Swelling upon boiling (%)
BPSH-35	25	15	41.2
Nafion 112	10	3.1	11.4

Conclusion

In situ chemical and mechanical stabilities and their dependence on temperature and humidity must be considered when evaluating membranes for PEM fuel cells. Though BPSH membranes showed poor chemical stability in ex situ Fenton tests, they outperformed Nafion 112 membranes in OCV decay and potential cycling tests with H_2/O_2 in fuel cell conditions. The superior in situ chemical stability exhibited by BPSH membranes is partly because of their lower gas-crossover rates than Nafion 112 membranes. Gas-permeation property plays an important role in membrane durability. Lower oxygen crossover rates to the anode result in lower anode peroxide formation rates, and lower hydrogen crossover rates to the cathode result in lesser Pt deposition inside the membrane. Though the correct mechanism for membrane degradation is not entirely known, the process seems to be a strong function of gas humidity and local water activity. Gas humidity affects the mechanical durability of the membranes, especially if the fuel cell operation calls for frequent start–stop cycles. The frequent wet-up and dry-out cycles cause mechanical stresses on the membrane. It is desirable for a membrane to have lower water uptake, which translates to better dimensional stability.

Acknowledgments

The U.S. Department of Energy supported this work under contract number DE-FC36-02A167608, for which the authors are grateful. The authors thank Professor James E. McGrath and his group at Virginia Polytechnic Institute and State University, Blacksburg, VA, for providing the hydrocarbon (BPSH-35) membranes, Dr. Ned Cipollini (United Technologies Research Center, Hartford, CT) for MEA development, Barbara LeTournea (UTRC) for MEA fabrication, Michael E. Fortin for fuel cell tests and RH cycling experiments, Darlene S. Mokrycki for water analysis, Paul Plasse for GDM fabrication, and Shruti Modi for Fenton tests.

University of South Carolina assisted in meeting the publication costs of this article.

References

1. DuPont Fuel Cells/Products and Services/Nafion Membranes and Dispersions, http://www.dupont.com/fuelcells/products/nafion.html (last accessed Nov 14, 2007).
2. J. P. Meyers, *DoE Hydrogen, Fuel Cells and Infrastructure Technologies Review*, May 2004.
3. M. A. Hickner, H. Ghassemi, Y. S. Kim, B. R. Einsla, and J. E. McGrath, *Chem. Rev. (Washington, D.C.)*, **104**, 4587 (2004).
4. J. A. Kerres, *J. Membr. Sci.*, **185**, 3 (2001).
5. J. J. Dumais, A. L. Cholli, L. W. Jelinski, J. L. Hedrick, and J. E. McGrath, *Macromolecules*, **19**, 1884 (1986).
6. A. Noshay and L. M. Robeson, *J. Appl. Polym. Sci.*, **20**, 1885 (1976).
7. F. Wang, M. Hickner, Y. S. Kim, T. A. Zawodzinski, and J. E. McGrath, *J. Membr. Sci.*, **197**, 231 (2002).
8. D. P. Wilkinson and J. St. Pierre, in *Handbook of Fuel Cells—Fundamentals, Technology and Applications, Fuel Cell Technology and Applications*, Vol. 3, W. Vielstich, H. A. Gasteiger, and A. Lamm, Editors, Chap. 43, John Wiley and Sons, Ltd., West Sussex, England, (2003).
9. C. Walling, *Acc. Chem. Res.*, **8**, 125 (1975).
10. J. Healy, C. Hayden, T. Xie, K. Olson, R. Waldo, M. Brundage, H. Gasteiger, and J. Abbott, *Fuel Cells*, **5**, 302 (2004).
11. G. Escobedo, T. H. Madden, and R. B. Moore, *DOE Hydrogen Program FY 2005 Progress Report*, p. 761, (2005).
12. T. Patterson, *Pre-Print Archive-American Institute of Chemical Engineers*, Spring National Meeting, New Orleans, LA, pp. 313–318, (2002).
13. S. Mitsushima, S. Kawahara, K. Ota, and N. Kamiya, *J. Electrochem. Soc.*, **154**, B153 (2007).
14. Toray Industries, Inc., TORAYCA, http://www.torayca.com/index2.html (last accessed Nov 14, 2007).
15. G. Lin and T. V. Nguyen, *J. Electrochem. Soc.*, **152**, A1942 (2005).
16. A. B. LaConti, M. Hamdan, and R. C. MacDonald, in *Handbook of Fuel Cells: Fundamentals, Technology and Applications*, Vol. 3, W. Vielstich, A. Lamm, and H. Gasteiger, Editors, p. 647, John Wiley and Sons, Chichester, England (2003).
17. S. D. Knights, K. M. Colbow, J. St-Pierre, and D. P. Wilkinson, *J. Power Sources*, **127**, 127 (2004).
18. E. Endoh, S. Terazono, H. Widjaja, and Y. Takimoto, *Electrochem. Solid-State Lett.*, **7**, A209 (2004).
19. V. A. Sethuraman, J. W. Weidner, A. T. Haug, S. Motupally, and L. V. Protsailo, *J. Electrochem. Soc.*, **155**, B50 (2008).
20. V. A. Sethuraman, J. W. Weidner, A. T. Haug, S. Motupally, and L. V. Protsailo, Abstract 1107, The Electrochemical Society Meeting Abstracts, Vol. 2006-1, Denver, CO, May 7–12, 2006; V. A. Sethuraman, J. W. Weidner, A. T. Haug, S. Modi, and L. V. Protsailo, Abstract 451, The Electrochemical Society Meeting Abstracts, Vol. 2006-2, Cancun, Mexico, Oct 29–Nov 3, 2006.
21. S. C. Yeo and A. Eisenberg, *J. Appl. Polym. Sci.*, **21**, 875 (1977).
22. T. Kyu and A. Eisenberg, in *Perfluorinated Ionomer Membranes*, A. Eisenberg and H. L. Yeager, Editors, *Amer. Chem. Soc. Symp. Ser.*, 180, Chapter 6, 79, A. C. S. Publications, Washington, DC (1982).
23. C. Huang, K. S. Tan, J. Lin, and K. L. Tan, *Chem. Phys. Lett.*, **371**, 80 (2003).
24. T. Sakai, H. Takenaka, and E. Torikai, *J. Electrochem. Soc.*, **133**, 88 (1986).
25. A. T. Haug and L. Protsailo, *J. Electrochem. Soc.*, Submitted.
26. A. Panchenko, Dipl.-Chem., Institute für Phzsikalische Chemie der Universität Stuttgart (2004).
27. A. Haug, S. Modi, S. Motupally, and L. Protsailo, *J. Electrochem. Soc.*, Submitted.
28. S. Cleghorn, J. Kolde, and W. Liu, in *Handbook of Fuel Cells—Fundamentals, Technology and Applications, Fuel Cell Technology and Applications*, Vol. 3, W. Vielstich, H. A. Gasteiger, and A. Lamm, Editors, p. 566, John Wiley and Sons, Ltd., West Sussex, England (2003).
29. P. J. Ferreira, G. J. la O', Y. Shao-Horn, D. Morgan, R. Makharia, S. Kocha, and H. Gasteiger, *J. Electrochem. Soc.*, **152**, A2256 (2005).
30. W. Bi, G. E. Gray, and T. F. Fuller, *Electrochem. Solid-State Lett.*, **10**, B101 (2007).
31. P. S. Fedkiw and W.-H. Her, *J. Electrochem. Soc.*, **136**, 899 (1989).
32. R. Liu, W.-H. Her, and P. S. Fedkiw, *J. Electrochem. Soc.*, **139**, 15 (1992).
33. H. Takenaka, E. Torikai, Y. Kawami, and N. Wakabayashi, *Int. J. Hydrogen Energy*, **7**, 397 (1982).
34. D. E. Curtin, R. D. Lousenberg, T. J. Henry, P. C. Tangeman, and M. E. Tisack, *J. Power Sources*, **131**, 41 (2004).
35. M. F. Mathias, R. Makharia, H. A. Gasteiger, J. J. Conley, T. J. Fuller, C. J. Gittleman, S. S. Kocha, D. P. Miller, C. K. Mittelsteadt, T. Xie, et al., *Electrochem. Soc. Interface*, **14**, 24 (2005).